Copyright iStockphoto.com/David Joyner

New GPS Signals

Aviation Grade

Chips Off the Block IIF

Civil aviation depends on augmentation systems that use monitors and complex algorithms to ensure that GNSS signals meet rigorous requirements for accuracy and integrity. This includes detecting any imperfection in the shapes of the broadcast chips that may lead to differential range errors across different receiver types. In this article, researchers in the United States and Germany offer their impressions of transmissions from the first GPS Block IIF satellite, including the new operational L5 signal.

InsideGNSS
GPS | GALILEO | GLONASS | COMPASS

R. ERIC PHELTS, GRACE XINGXIN GAO, GABRIEL WONG, LIANG HENG, TODD WALTER, PER ENGE,
STANFORD UNIVERSITY

STEFAN ERKER, STEFFEN THOELERT, MICHAEL MEURER
GERMAN AEROSPACE CENTER (DLR)

While the GNSS community at large looks forward to the addition of any new generation of navigation satellites, the first Block IIF satellite — launched in May 2010 and designated space vehicle number (SVN) 62 — marks an especially important step forward for the aviation community. Non-aviation applications may take advantage of GNSS receivers that use any and all available ranging sources. However aviation requires signals operating in designated safety-of-life aeronautical radionavigation service (ARNS) bands to avoid interference from overlapping signals.

GPS L1 operates in a designated ARNS band, but L2 does not. The new L5 signal — the first operational version of which has begun transmitting on a test basis recently — is also in an ARNS band. And, as with L1, L5 can be used for aviation.

Because aviation users must meet rigorous safety-related standards, they need to rely only on signals that meet strict criteria for performance and reliability. This often translates into demands for ensuring robust performance and high availability of service while having fewer ranging sources upon which it can rely.

One area of concern is imperfection in the shapes of the broadcast chips that may lead to differential range errors across different receiver types. This article focuses on an evaluation of the new signals' chip shapes and their potential effect for aviation users.

Satellite-based navigation signals used for aviation must originate from well-established and trustworthy sources, such as GPS. Although other satellite navigation systems exist or are under development, none has gained the pedigree that GPS has earned from years of continued operation and dependable performance.

New GNSS signals — including GPS L5 — planned for use in aviation applications must demonstrate that they perform as well as those in the legacy constellation. And these new ranging sources must be monitored by the same systems that have guaranteed the integrity of the existing constellation.

Moreover, seamless integration of new signals into space-based and ground-based augmentation systems (SBAS and GBAS) requires that these signals meet the additional technical and operational standards for such systems, which have been achieved by the existing signals.

As we will see, the nominal deformation of the satellites L1 and L5 chips are within specifications and are compatible with existing satellites.

SVN 62 and Signal Deformation Monitoring

In their quest to validate the new Block IIF satellite, scientists, engineers, and aviation regulatory officials must answer the fundamental question, "How do the new signals compare to the others?"

When significant differences between the transmitted chip shapes exist from satellite-to-satellite, we refer to such differences as *signal deformations*. These deformations can lead to receiver range errors that vary as a function of receiver discriminator and filter characteristics.

In turn, such ranging errors must either be corrected by the augmentation system, if possible, or modeled and accounted for in the error analyses implemented by system operators. In extreme cases, an aberrant signal is flagged as unusable by an integrity monitor.

SBAS and GBAS currently employ signal deformation monitors to detect and exclude range sources that differ significantly from the other satellites. The assumptions made about nominal signal deformation have further implications for system performance. Non-aviation applications are often able to measure performance as a blend of the worst- and best-performing signals, but augmentation system performance is frequently determined by the worst possible combination of range sources. This can often translate into a decrease of system availability and, hence, utility for all aviation users.

To evaluate the signals being transmitted from SVN 62, we need to ensure that they are compatible with the monitors. We would like to be certain that existing assumptions made in SBAS and GBAS systems about the types of signal distortions encountered in existing GPS satellites also apply to this new satellite.

More specifically, we want to be confident that the code chips transmitted from SVN 62 have the same shape and duration as others measured in the past. Furthermore, we would like these properties to be independent of elevation angle. A previous satellite — SVN

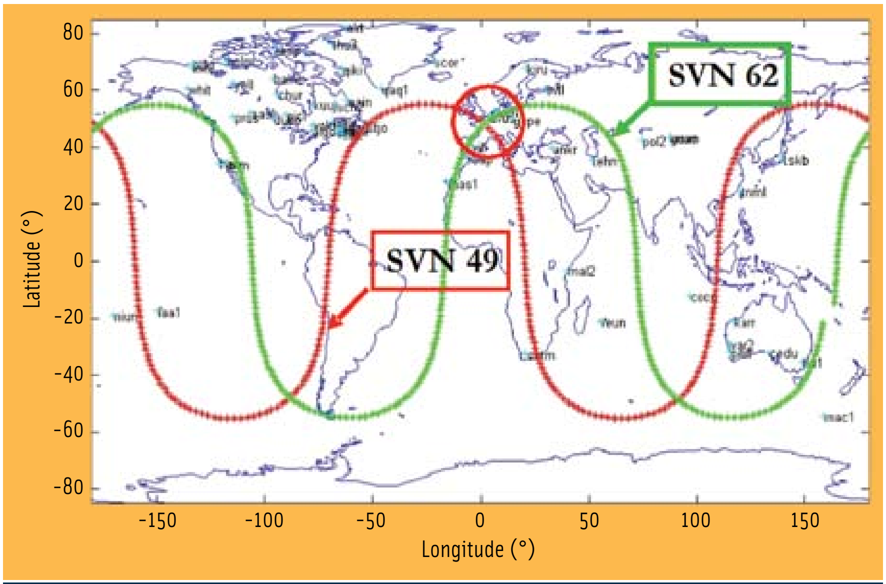

FIGURE 1 Ground tracks of SVN 49 and SVN 62. The receivers shown on this map are the 69 out of 300+ IGS sites that output both SVN 49 and SVN 62 measurements as of Day 170, Year 2010.

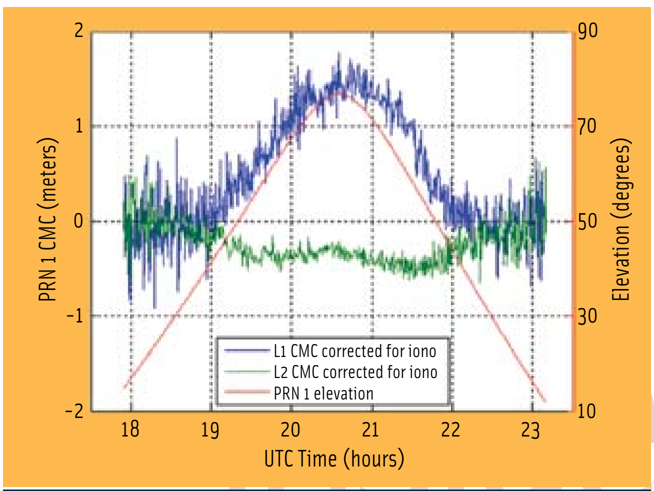

FIGURE 2 SVN 49 code-minus-carrier measurements after applying a dual-frequency ionosphere correction. The clock, orbit, troposphere, and ionosphere errors are all eliminated. An obvious positive elevation-dependent bias exists in the L1 C/A measurements. A slight negative elevation-dependent bias is seen in the L2 measurements.

49 — violated thislatter property; so, it is important to verify its performance in SVN 62 early, before proceeding with more detailed analysis.

SVN 49 Elevation Angle Dependence

In early 2009, the navigation community got its first look at an L5 signal transmitted from a GPS satellite—SVN 49. The Block IIRM satellite had been retrofitted with an L5 transponder to temporarily reserve the spectrum for signals planned for implementation on the upcoming Block IIF satellites. Unfortunately, that retrofit had the unintentional side-effect of introducing an internal reflection onto the L1 signal.

The details of this reflected signal have been studied and documented extensively by others, but the effect is significant to SBAS and GBAS. The transmitted signal is internally distorted by multipath. Worse yet, this distortion created ranging errors that vary as a function of user receiver implementation and elevation angle.

This elevation-dependent variation is can be particularly problematic for SBAS, which must protect the integrity of many different users observing the satellite from a wide range of elevation angles.

Does an elevation dependent bias also exist for SVN 62? To answer this question, we processed data from the International GNSS Service (IGS) network to compare the elevation angle dependence of the two satellites. The same IGS site was used for both SVN 49 and SVN 62 in our study so that the receiver errors are comparable for each. The IGS site was selected based on the following requirements:

1. The receiver outputs measurements for both SVN 49 and SVN 62 satellites. As both satellites are currently set "unhealthy," many IGS sites do not output measurements for them. We screened all 300+ receivers in the IGS network and found that only 69 of them provided data for both satellites as of Day 170, Year 2010.
2. The receiver observes both SVN 49 and SVN 62 at high elevation angles. As we evaluate elevation-angle dependency, we want the full, or near-full, span of the elevation. **Figure 1** shows the ground tracks of the two satellites. We favored receivers located in the vicinity of the cross point marked by a red circle.
3. The receiver noise is low. The two nearest IGS receivers to the ground track cross point are "brus" (Brussels, Belgium) and "wsrt" (Westerbork, the Netherlands). We choose "wsrt" for investigation. Although only the second-nearest site, its receiver noise and multipath is lower than 'brus' based on our study. The longitude, latitude, and height of the site are +4.3592 degrees longitude, +50.7978 degrees latitude, and 149.7 meters (above geoid) respectively.

The elevation-angle effect was readily apparent on the measurements of SVN 49 recorded on June 19, 2010, and presented in **Figure 2**. (This bias was further verified by checking the data from other IGS sites and NSTB sites.) It shows the code/carrier difference for a single frequency after applying dual-frequency carrier-based ionosphere error corrections. Clock, orbit, troposphere, and ionosphere errors are all removed.

The figure indicates that the SVN 49 anomaly is primarily in the L1 band; the code-minus-carrier (CMC) with ionosphere correction for PRN 1 has a bias highly correlated with satellite elevation. The bias has a relative shift of 1.5 meters between a low elevation angle of 15 degrees and a high elevation of 77 degrees. The L2 CMC curve is flatter,

GNSS
GPS | GALILEO | GLONASS | COMPASS

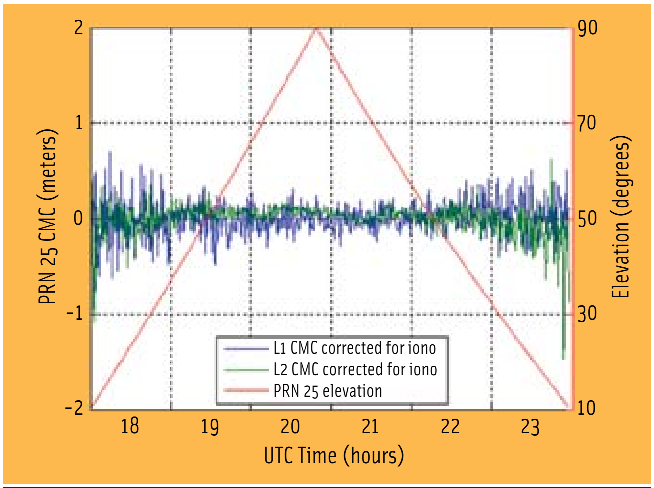

FIGURE 3 SVN 62 code-minus-carrier measurements after applying a dual-frequency ionosphere correction. The clock, orbit, troposphere, and ionosphere errors are all eliminated. No apparent elevation-dependent bias exists in either L1 or L2 measurements.

although apparently with a bias of about 0.4 meters in the opposite direction.

Figure 3 shows a similar plot for the L1 signal on SVN 62 and reveals no noticeable error dependence on elevation angles from 10 to 89 degrees.

SBAS and GBAS Models for Signal Deformation

Assuming no internal reflections or elevation angle dependencies, SBAS and GBAS generally classify potential signal deformations into two types: digital and analog. *Digital distortions* occur when timing of the individual chip transitions of the transmitted codes vary from ideal. They are modeled as either an advance or delay of the rising or falling edge of a C/A code chip and can create "dead zones" (i.e., plateaus) atop an ideal correlation peak. (See **Figure 4**.)

The following sections compare both types of nominal deformations for the SVN 62 to those measured for the legacy constellation of satellites.

Analog deformations result from filter limitations in either the signal transmission path or the receiver hardware. Theses create oscillations that cause the correlation peak to become asymmetric, as illustrated by **Figure 5**.

To characterize either type of distortion requires high-gain, high-resolution measurements of the transmitted signals. The basic technique for measuring digital code distortions is to compute successive differences between the ideal code chip width and the measured ones for each PRN. (One of this artcle's authors, Gabriel Wong, will present a more detailed discussion of these techniques and a completed summary of digital distortions at the September ION GNSS-2010 conference in Portland, Oregon, in September.)

The first measurement of this type was published in 2004. (See the paper by A. Mitelman cited in the Additional Resources section near the end of this article). **Figure 6** summarizes that work by plotting digital distortion results for L1 C/A code as a function of GPS space vehicle numbers (SVN) shown in chronological order of launch date. That study revealed that the largest distortions were observed on the Block IIR satellites.

Figure 7 provides more recent estimates for digital distortion for L1 C/A code on 17 SVs using data taken from between 2008 and 2010. The estimates are fairly consistent with previous findings, confirming that the Block IIR satellites continue to possess the largest amount of digital distortion, while the Block II-RM SVs tend to have much smaller digital distortion.

The L1 C/A-code digital distortion on the first Block IIF SVN 62 is comparable to that of the Block IIR-M satellites. Both have digital distortion estimates on the order of 1–1.5 nanoseconds.

However, the SVN 62 distortion is significantly larger for the L5 signal — approximately 6 nanoseconds for the in-phase code component and slightly more than 4 nanoseconds for the quadrature component. (The standard deviation of these measurements is approximately 0.25 nanoseconds for the Block IIA and IIR SVs and slightly higher for the Block IIR-M and IIF SVs.) Somewhat unexpectedly, we find that the digital distortion estimates differ so much amongst signals from the same satellite.

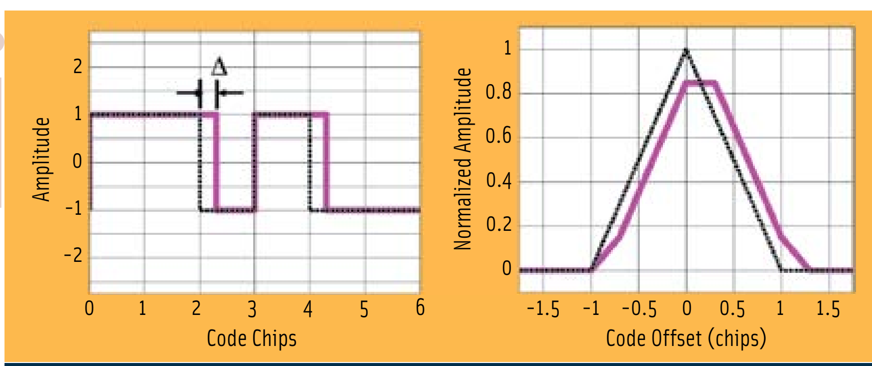

FIGURE 4 Example of digital code distortion model and its effect on the correlation peak

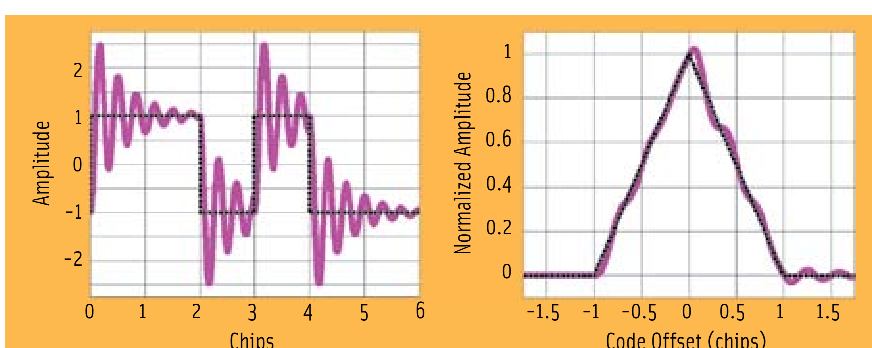

FIGURE 5 Example of analog code distortion model and its effect on the correlation peak

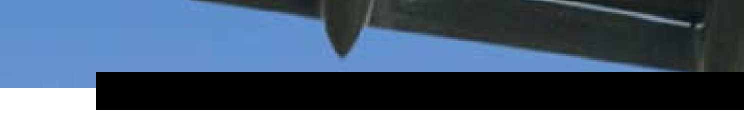

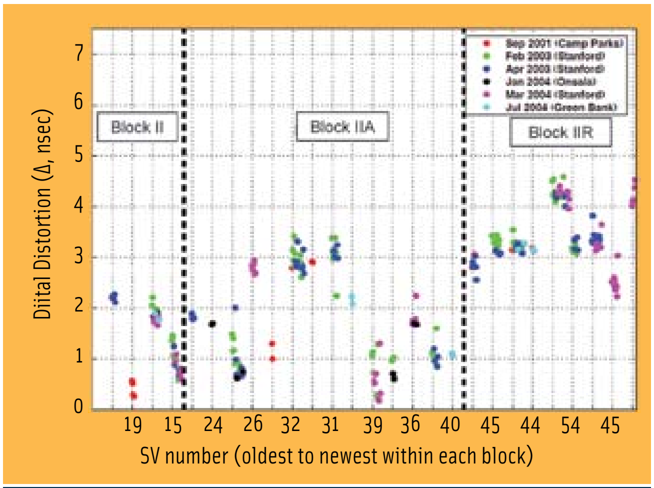

FIGURE 6 Historical digital distortion plotted as a function of SVN, from earliest to latest launch date (from A. Mitelman)

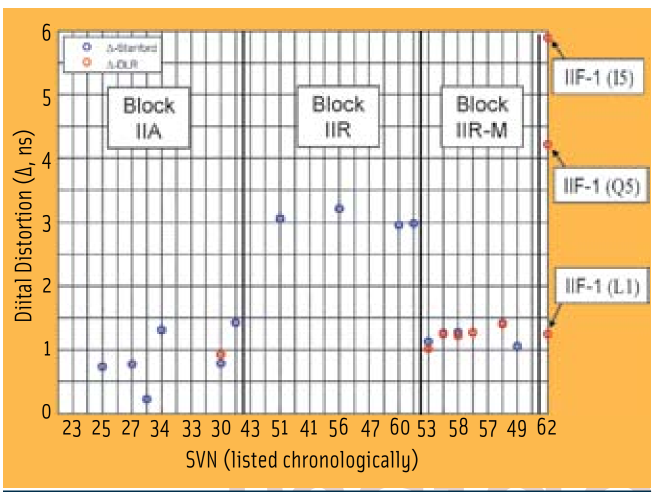

FIGURE 7 Recent digital distortion summary plotted as a function of SVN (from earliest to latest launch date). This uses data taken between June 2008 and 2010. Three results appear for SVN 62 signals: one each for L1 C/A code, I5 (L5, In-phase), and Q5 (L5, quadrature).

Figure 8 compares the C/A-code chip shapes, or step-responses, for the GPS SVs represented in Figure 7. It can be seen that all the responses for all the SVs are fairly similar. Each has an overshoot ranging from about 110 to 120 percent of the steady-stare amplitude, and the overshoot for SVN62 lies approximately in the middle of this range. (The maximum overshoot corresponds to SVN56, and the minimum corresponds to SVN58.)

The step response for SVN62 does, however, seem to be more damped. Its settling time appears significantly smaller than for the other responses.

Figure 9 compares the step responses of the L1 C/A and two L5 codes on SVN 62. In order to better compare the effects of the filter after transition, segments of the L5 code that had five positive chips in row were selected for display in the figure. Thus, what is shown is five times longer than a single L5 chip width.

As expected, the two L5 signals agree quite closely with each other. Ideally, these would be identical since all the signals pass

GNSS Solutions®

Tutorials Prior to ION GNSS 2010
Sept. 20-21, 2010, Portland, OR, USA

24 High-Quality Tutorials; 5 tracks:

Track 1:
• CN405 GNSS I, Dr. Chris Bartone, Ohio Univ.
• CN406 GNSS II, Dr. Chris Bartone, Ohio Univ.
• CN420 GPS Modernization, Tom Stansell
• CN428 Glonass, Dr. Sergey Revnivykh & others
• CN360 IP and Patents, Dr. Gary Edwards, J.D., Steve Levitan, J.D., Haynes and Boone

Track 2:
• CN425 Future GNSS Signals & Systems, Dr. Tony Pratt, Obstar
• CN426 Future GNSS Signal Performance, Dr. Tony Pratt, Obstar
• CN413 GNSS RAIM & Integrity, Dr. Christophe Macabiau, ENAC
• CN433 Receiver Signal Processing for Future GNSS Signals I, Dr. Oliver Julien, ENAC
• CN434 Receiver Signal Processing for Future GNSS Signals II, Dr. Oliver Julien, ENAC

Track 3:
• CN431 GNSS Receiver Design I: RF Front-end, Dr. Sanjeev Gunawardena, Ohio University
• CN432 GNSS Receiver Design II: Baseband, Dr. Sanjeev Gunawardena, Ohio University
• CN435 GNSS Receiver Vector Tracking, Dr. Matthew Lashley, Navigation Tech. Assoc.
• CN441 GNSS Antennas I, Dr. Bartone, Ohio Univ.
• CN445 GNSS Antennas II, Dr. Bartone, Ohio Univ. & Dr. Jiti Gupta, Ohio State University

Track 4:
• CN460 Intro. to Strapdown INS I, Dr. Kevin Dutton, Honeywell International
• CN461 Intro. to Strapdown INS II, Dr. Kevin Dutton, Honeywell International
• CN473 Land Navigation - Integrated, Dr. David Bevly, Auburn University
• CN462 Apps. of Inertial Navigation I, Dr. Andrey Soloviev, University of Florida
• CN463 Apps. of Inertial Navigation II, Dr. Andrey Soloviev, University of Florida

Track 5 (Dr. Mohinder Grewal, CSU-Fullerton):
• CN480 Kalman Filter for GPS/INS Integration I
• CN481 Kalman Filter for GPS/INS Integration II
• CN482 GPS/INS Integration I
• CN483 GPS/INS Integration II

Quality you can count on.
Check them out . . .

www.GNSSsolutions.com/tutorials.html
740-591-1660 info@GNSSsolutions.com
!! Sign Up Today !!

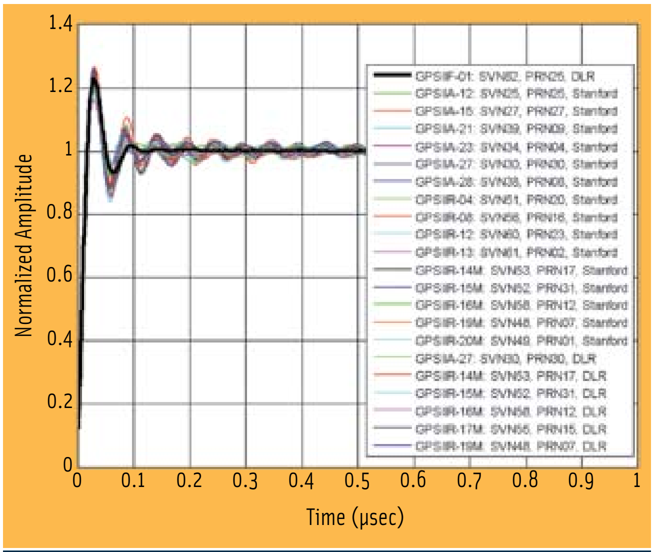

FIGURE 8 Comparison of the step responses on the L1 C/A codes of 17 GPS satellites. The response of SVN62 is depicted by the heavy black trace.

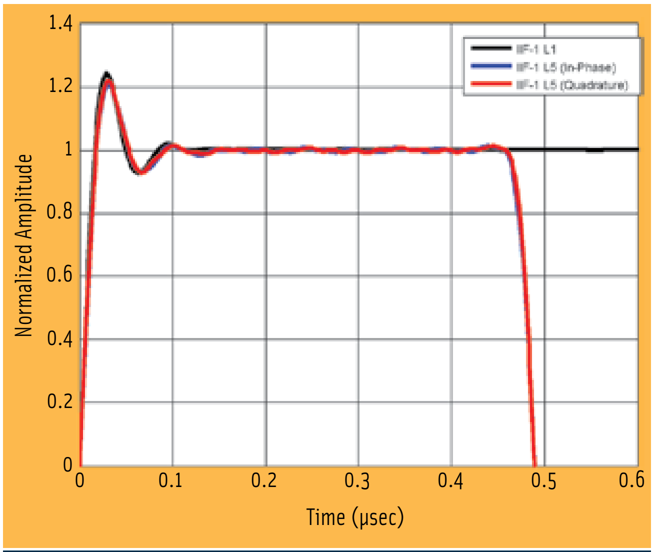

FIGURE 9 Comparison of the step responses on three codes transmitted from SVN 62: L1 C/A (black), L5 in-phase (blue) and quadrature (red).

through the same filtering components on the satellite. However, some small differences can be seen. Measurement error may account for some of the differences observed. The L1 C/A signal shape is quite similar to the L5 response, which indicates similar filter designs in the two different frequency paths.

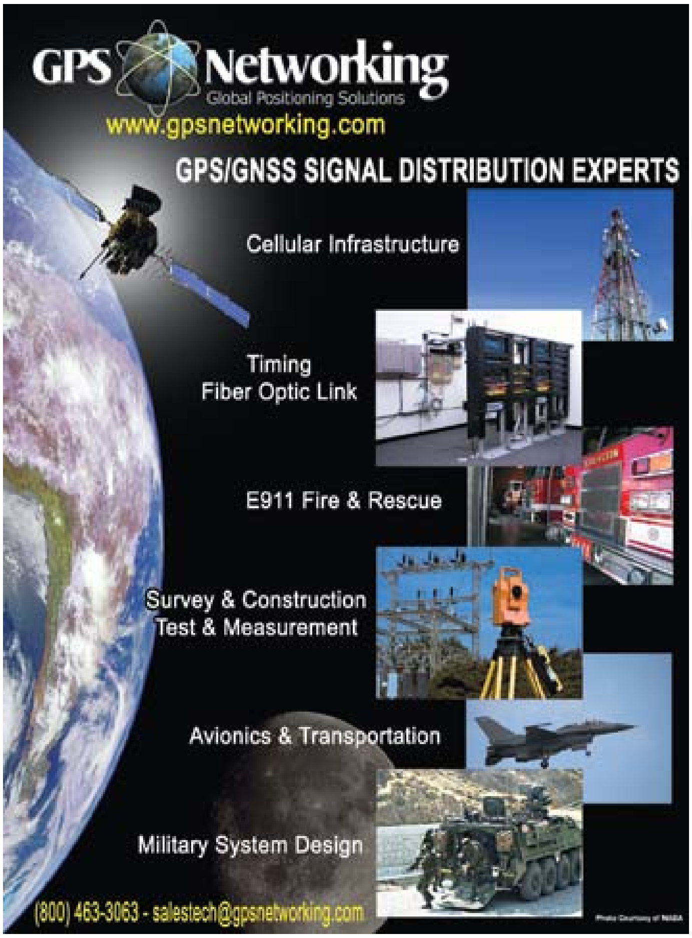

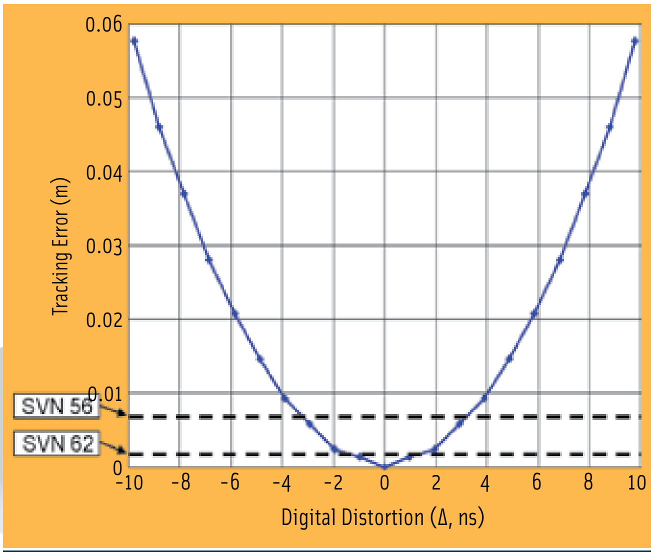

FIGURE 10 Modeled WAAS user tracking errors on L1 C/A code due to digital distortion only. Errors have been differentially corrected by the WAAS reference station receiver (Early-minus-late discriminator at 0.1-chip spacing and a filter having 18MHz bandwidth). User receiver properties are modeled according to the constraints defined in the Minimum Operational Performance Standards (MOPS) DO-229D (RTCA, Inc.).

Range Errors Due to Signal Deformations

If only digital distortion were present, the range errors would be relatively small. For example, **Figure 10** shows the results for $-10 \le \Delta \le 10$ nanoseconds on L1 C/A code, assuming all users of the Wide Area Augmentation System (WAAS, the U.S. SBAS) have early-minus-late (EML) discriminators. For the SVs discussed in this article, the largest range error due to nominal digital distortion alone would be less than one centimeter. For SVN 62, it would be less than two millimeters.

This simplified analysis does not account for the analog distortion effects observed in Figures 8 and 9, however. Also, this analysis does not account for the fact that true range errors

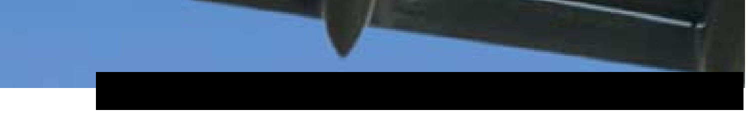

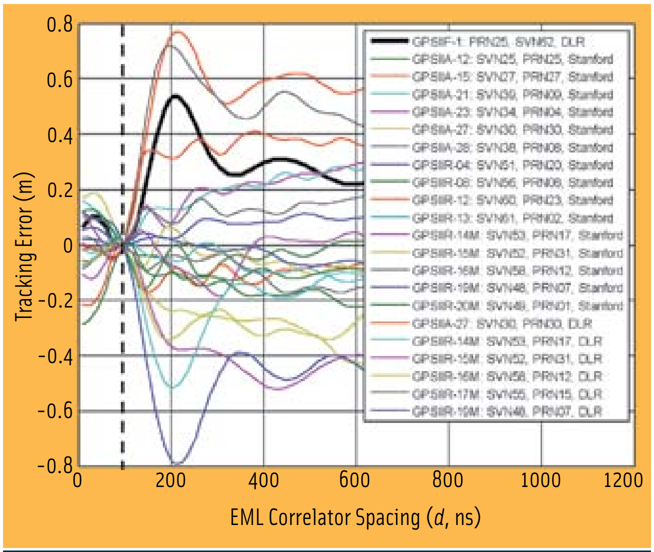

FIGURE 11 Tracking errors of all satellites relative to mean across all satellites plotted as a function of Early-Minus-Late (EML) correlator spacing, d.

result from tracking error differences between the actual satellites signals — which are never completely ideal.

For an actual set of range sources, the analog and digital distortions combine. They both deform the correlation peak. A receiver subsequently processes and estimates tracking errors on these distorted peaks. The range error due to signal deformations is determined by the tracking error on any individual signal made relative to the others.

The relative nominal signal deformation performance for all satellites can be found by forming correlation peaks from the measured codes of signals from different SVs and then finding the early-minus-late (EML) tracking errors across a range of correlator spacings. Ideal, perfectly symmetrical peaks would produce results independent of correlator spacing. However, actual signals produce estimates that vary with correlator spacing. Signal deformation causes these variations to differ from satellite-to-satellite.

Figure 11 computes relative tracking errors for the previously discussed SVs assuming early-minus-late (EML) tracking and wide bandwidths greater than 30 megahertz. Because variations common across all satellites do not create a differential error, an average, common-mode distortion effect has been removed.

The reference correlator spacing assumed here is 0.1-chip (~100 nanosecond), consistent with the current WAAS reference receiver configuration. Because no additional filtering or receiver processing has been applied here, all the traces have zero relative error by definition at that spacing.

Given a 100-nanosecond reference correlator spacing, the largest range errors due to signal deformation may occur for users who have wider correlator spacings. This is consistent across all the satellites — including SVN 62. The trace corresponding to SNV 62, although not in the middle, is not at either extreme in this grouping. At the narrowest spacing of approximately 50 nanoseconds, the worst-case difference in range error (defined as maximum error minus minimum error)

across all traces is approximately 50 centimeters. The range error is about 10 centimeters for SVN 62 at this spacing.

The largest differences occur around 200 nanoseconds, where the worst difference in range error approaches 1.6 meters. The range error for SVN 62 is about 0.55 meters at that offset. These results indicate that the L1 C/A code on SVN 62 conforms to the deformation status of the existing constellation and likely introduces minimal additional nominal deformation biases of concern.

Conclusions

The L1 C/A code on SVN 62 appears to meet or exceed expectations with respect to signal deformations. We do not observe any noticeable elevation angle dependence. With an estimated digital distortion of only about 1.25 nanoseconds, the L1 C/A code appears to be among the highest quality signals in terms of digital distortion.

Also, this signal seems nearly prototypical in terms of nominal analog distortion since the transient effects — such as overshooting, rise time, peak time, and settling time — are essentially at the center of the others. In fact, the SVN 62 L1 C/A-code signal's analog step response seems superior in that the transients dampen more quickly than those observed in the other SVs.

The relative range errors also appear to be within the bounds established by the other satellites measured thus far. All these factors indicate that the L1 C/A code on SVN 62 is a good signal and suitable for use by aviation. More specifically, the observed nominal signal deformations are compatible with the existing monitors and assumptions employed by WAAS and LAAS (or local area augmentation system, the U.S. version of SBAS).

The L5 codes are more difficult to conclusively assess for aviation. Because SVN 62 provides the first true GPS L5 signal and SBAS or GBAS L5 signal deformation monitors do not currently exist; we have made relatively few assumptions about its L5 signal.

Larger digital distortions were observed on the L5 codes, but this does not necessarily imply the signal is anomalous. And although the analog distortion on L5 corresponds well with those observed on the L1 C/A code, this alone does not imply the signal is well-behaved. Each of these results needs to be compared against other GPS L5 signals to make a true assessment of the quality of any individual signal.

Finally, we should note that at the time of writing of this paper, SVN 62 had only recently begun broadcasting. The U.S. Air Force operators had not completed their signal testing for the spacecraft; so, these results may not represent the final operational configuration of the satellite.

Still, this first look at the the L1 chips causes us to be optimistic about the immediate utility of this new satellite for GBAS and SBAS. Our first look at L5 indicate chip quality very similar to previous measurements for L1. However, the L5 signal is new, and deeper investigations are ongoing.

GPS | GALILEO | GLONASS | COMPASS

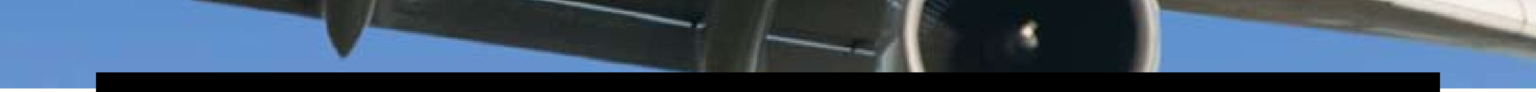

Hardware Description

Many of the high-gain measurements used for the analyses discussed in this article were taken using the 46-meter parabolic dish antenna at Stanford University and operated by Stanford Research Institute. The antenna achieves a 45-decibel gain and also incorporates a 50-decibel low-noise amplifier ($T_{eq} \approx$ 40K). It has a 50-megahertz bandwidth over the L-band. (See Figure 4.)

This is the same antenna that was used to take the code distortions measurements in Figures 7, 8, 9, 10 and 12. The antenna and hardware used for the DLR measurements are described in the article entitled "On the Air: New Signals from the First GPS IIF Satellite" in this issue of *Inside GNSS*.

Acknowledgments

The authors gratefully acknowledge the support of the Federal Aviation Administration under CRDA 2000G028. This article contains the personal comments and beliefs of the authors and does not necessarily represent the opinion of any other person or organization.

Manufacturers

The IGS site at Westerbork has an **Allen Osborne Associates** (now ITT) TurboRogue SNR-12 receiver. Stanford researchers use an Agilent 89640 Vector Signal Analyzer (VSA) from **Agilent Technologies**, Santa Clara California, USA. The data was processed by a software radio GNSS receiver. This receiver and the specialized signal authentication codebase are implemented in MATLAB from the **MathWorks, Inc.**, Natick Massachusetts, USA.

Additional Resources

[1] Hegarty, C. J., and E. Chatre E., "Evolution of the Global Navigation Satellite System (GNSS)," *Proceedings of the IEEE,* Vol. 96, Issue 12, December 2008

[2] Mitelman, A. M., *Signal Quality Monitoring For GPS Augmentation Systems,* Ph.D. Thesis, Stanford University, Stanford, California, 2004

[3] RTCA, Inc., *Minimum Operational Performance Standards (MOPS) for WAAS,* DO-229D

[4] Spilker, J. J., and A. J. Van Dierendonck, A. J., "Proposed New Civil GPS Signal at 1176.45 MHz," *Proceedings of the 12th International Technical Meeting of the Satellite Division of the Institute of Navigation (ION GPS-1999)* September 1999

[5] Spilker, Jr., J. J., and A. J. Van Dierendonck, "Proposed New L5 Civil GPS Codes," *Navigation Journal,* Vol. 48, No. 3, Institute of Navigation, 2001

[6] Van Dierendonck, A. J., and J. J. Spilker Jr. , "Proposed Civil GPS Signal at 1176.45 MHz: In-Phase/Quadrature Codes at 10.23 MHz Chip Rate," *Proceedings of ION Annual Meeting,* 1999

[7] Wong, Gabriel (2010). "Measuring Digital Signal Deformations on GNSS Signals," (forthcoming) *Proceedings of Institute of Navigation, Global Navigation Satellite Systems (ION GNSS-2010),* Portland, Oregon, September 2010

Authors

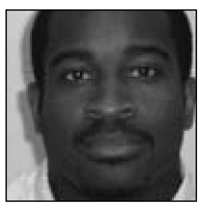

R. Eric Phelts, Ph.D., is a research engineer in the Department of Aeronautics and Astronautics at Stanford University. He received his B.S. in mechanical engineering from Georgia Institute of Technology, and his M.S. and Ph.D. in Mechanical Engineering from Stanford University. His research involves signal deformation monitoring techniques and analysis for SBAS, GBAS, and the GPS Evolutionary Architecture Study (GEAS).

Grace Xingxin Gao, Ph.D., is a research engineer in the GPS lab of Stanford University. She received the B.S. degree in mechanical engineering and the M.S. degree in electrical engineering, both at Tsinghua University, Beijing, China. She obtained the Ph.D. degree in electrical engineering at Stanford University. Her current research interests include GNSS signal and code structures, GNSS receiver architectures, and interference mitigation. She has received the Institute of Navigation (ION) Early Achievement Award.

Gabriel Wong is an Electrical Engineering Ph.D. candidate at the Stanford University GPS Research Laboratory. He has previously received an M.S.(EE) from Stanford University, and a B.S.(EECS) from UC Berkeley. His current research involves signal deformation monitoring for GNSS signals.

Liang Heng is a Ph.D. candidate under the guidance of Professor Per Enge in the Electrical Engineering Department at Stanford University. He received the B.S. and M.S. degrees in electrical engineering from Tsinghua University, Beijing, China. His current research interests include GNSS signal processing and GPS modernization.

Todd Walter, Ph.D., is a senior research engineer in the Department of Aeronautics and Astronautics at Stanford University. He received his Ph.D. from Stanford and is currently working on the Wide Area Augmentation System (WAAS), defining future architectures to provide aircraft guidance, and working with the U.S. Federal Aviation Administration and GPS Wing on assuring integrity on GPS III. Key early contributions include prototype development proving the feasibility of WAAS, significant contribution to WAAS MOPS, and design of ionospheric algorithms for WAAS. He is a fellow of the Institute of Navigation.

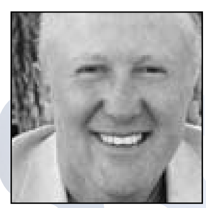

Per Enge, Ph.D., is a professor of aeronautics and astronautics at Stanford University, where he directs the GNSS Research Laboratory. He has been involved in the development of the Federal Aviation Administration's GPS Wide Area Augmentation System (WAAS) and Local Area Augmentation System (LAAS). Enge received his Ph.D. from the University of Illinois. He is a member of the National Academy of Engineering and a Fellow of the IEEE and the Institution of Navigation.

Note: *The biographies for the DLR co-authors can be found at the end of the previous article on page 35.* IG